NSF GRANT # 0219123
GEOMECHANICS & GEOMATERIALS

Integrated Tools for Predicting, Monitoring and Controlling Ground Movements due to Excavations

Richard J. Finno, PhD, PE
Professor, Department of Civil and Environmental Engineering, Northwestern University, Evanston, IL 60208, r-finno@northwestern.edu

Youssef M.A. Hashash, PhD, PE
Professor, Department of Civil and Environmental Engineering, University of Illinois at Urbana-Champaign, Urbana, IL, hashash@illinois.edu

Abstract: This paper describes developments of integrated tools for predicting, monitoring, and controlling ground movements associated with excavations in urban areas. Successful use of monitoring data to update performance predictions of supported excavations depends equally on reasonable numerical simulations of performance, the type of monitoring data used as observations, and the optimization techniques used to minimize the difference between predictions and observed performance. This paper summarizes each of these factors and emphasizes their inter-dependence. Numerical considerations are described, including the selection of the type of finite element formulation, the initial stress conditions with emphasis on urban environments, the importance of reasonable representation of the construction process, and factors affecting the selection of the constitutive model. Monitoring data that can be used in conjunction with current numerical capabilities are discussed, including laser scanning and webcams for developing an accurate record of construction activities, and automated and remote instrumentations to measure movements. Intelligent, self-updating numerical models that have been successfully used to compute anticipated ground movements, update predictions of field observations and to learn from field observations are summarized. Integration of heterogeneous data using a GIS based system is discussed. Example applications of these techniques from case studies are presented to illustrate the capabilities of this approach.

1. Introduction: With new development, and increasingly more redevelopment, within urban areas there is a clear need to efficiently and safely develop underground space. A major concern when placing deep excavations in urban environments is the impact of construction-related ground movements on adjacent buildings and utilities. In practice, when designers are faced with an excavation where ground movements are a critical issue, they can estimate movements using semi-empirical methods or results of numerical modeling. While numerical simulations have become more common to analyze ground response to excavations as part of the design process, finite element predictions contain uncertainties related to soil properties, support system details, and construction procedures. If one wants to predict and subsequently evaluate the overall performance of a design, a procedure that incorporates an evaluation of the results of the predictive analysis must be defined. The procedure to accomplish this task is usually referred to as the "observational method" (Peck, 1969), a framework wherein construction and design procedures and details are adjusted based upon observations and measurements made as construction proceeds. While the observational method is conceptually very helpful, it is quite difficult to use observed movements for controlling construction in a timely enough fashion to be of use in a typical excavation project, where time is of the essence to a contractor, or to judge quantitatively how well the work is proceeding.

While it is common to include a monitoring program during construction to record the ground movements, structural responses of the support system, and, in some cases, adjacent building movements, it is rare that these observations are used to control the construction process and update predictions of movements given the measured deformations at early stages of construction. Whereas significant developments have been made in the acquisition of field data, efforts to integrate various components of data acquisition and prediction of deformations have had limited success due to difficulty of the problem and the presence of several missing links to complete the deformation construction cycle illustrated in Figure 1. Furthermore, many factors affect the ground movements caused by excavations, including stratigraphy, soil properties, support system details, construction activities, contractual arrangements and workmanship.

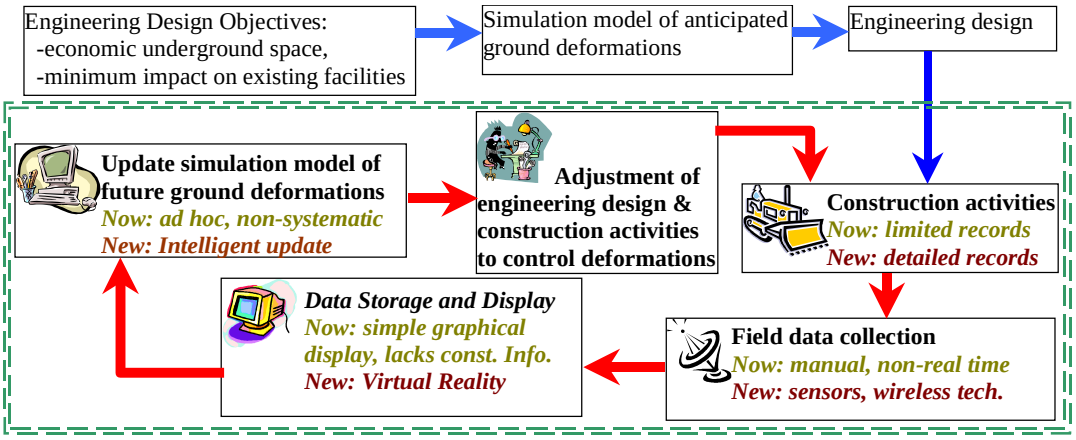

Figure 1: Deformation control cycle during deep excavations.

This paper describes developments of integrated tools for predicting, monitoring, and controlling ground movements associated with excavations in urban areas. The goal of such tools is to allow one to use the observed performance at early stages of a project to objectively calibrate a predictive model so that reliable predictions of subsequent performance can be made. The successful application of such techniques depends on the predictive model, in this case a finite element simulation of construction, the monitoring data and the inverse technique itself. This paper will illustrate these points by examining the technique as applied to supported excavations made through soft to medium clays. Comments are made regarding how details of the finite element simulations, the instrumentation and data collection, and the inverse technique affect the results of the methodology. Several examples of excavations where these techniques were applied are presented.

2. Finite Element Predictions of Excavation Performance: A key to a successful finite element simulation is to reasonably represent within a numerical simulation pertinent field activities during construction. In addition to replicating construction procedures and dimensionality of the problem, one must also carefully consider the applicability of a constitutive model to replicate the aspects of behavior that most affect the measurements that one makes to evaluate performance.

2.1. Representing Field Conditions in Finite Element Simulations: While supported excavations commonly are simulated numerically by modeling stages of excavation and support installation, it is necessary to simulate all aspects of the construction process that affect the stress conditions around the excavation to obtain an accurate prediction of behavior. This may involve simulating previous construction activities at the site, installation of the supporting wall and any deep foundation elements, as well as the removal of cross-lot supports or detensioning of tiedback ground anchors. Furthermore, issues of time effects caused by hydrodynamic effects or material responses may be important.

Finno and Tu (2006) summarized the effects of a number of key numerical assumptions, and corresponding appropriate techniques, on the computed performance of supported excavations. First the manner in which the excavation is simulated including the removal of soil elements in a finite elements mesh should satisfy the principal of superposition as described by Ghaboussi and Pecknold (1985). Other key assumptions include selecting appropriate drainage conditions during excavation (Clough and Mana 1976; O'Rourke and O'Donnell 1997; Whittle et al. 1993), starting with appropriate initial effective stresses that include the effects of past construction activities at a site (Calvello and Finno 2003), and accurately defining the initial ground water conditions for a site (e.g. Finno et al. 1989). Many times the effects of the installation of a wall are ignored in a finite element simulation and the wall is "wished-into-place" with no change in the stress conditions in the ground or any attendant ground movements. However, there is abundant information (e.g. Clough et al. 1989; O'Rourke and Clough 1990; Finno et al. 1988; Sabatini 1991; Koutsoftas et al. 2000) that shows ground movements may arise during installation of the wall, and, if ignored, these may have a significant impact on the accuracy of the computed responses, particularly in cases where the resulting ground deformations are relatively small. One must take care when representing the bracing system in a model. In typical plane strain simulations, application of prestress for cross-lot braces and installation of tiedback ground anchors can present problems under certain circumstances (e.g. Finno and Tu 2006).

Figure 2 illustrates some of the challenges of using field observations to calibrate numerical models of any kind, even when detailed records exist. This figure summarizes the construction progress at the Chicago-State excavation (Finno et al 2002) in terms of

excavation surface and support installation on one of the walls of the excavation for selected days after construction started. Also shown are the locations of two inclinometers placed several meters behind the wall. If one is making a computation assuming plane strain conditions, then it is clear that one must judiciously select a data set so that planar conditions would be applicable to a set of inclinometer data. If one is using an integrated approach wherein data is collected and compared with numerical predictions in almost real time, then it is clear that a 3D analysis would be required for most days as a result of the uneven excavated surface and timing of the anchor prestressing operations.

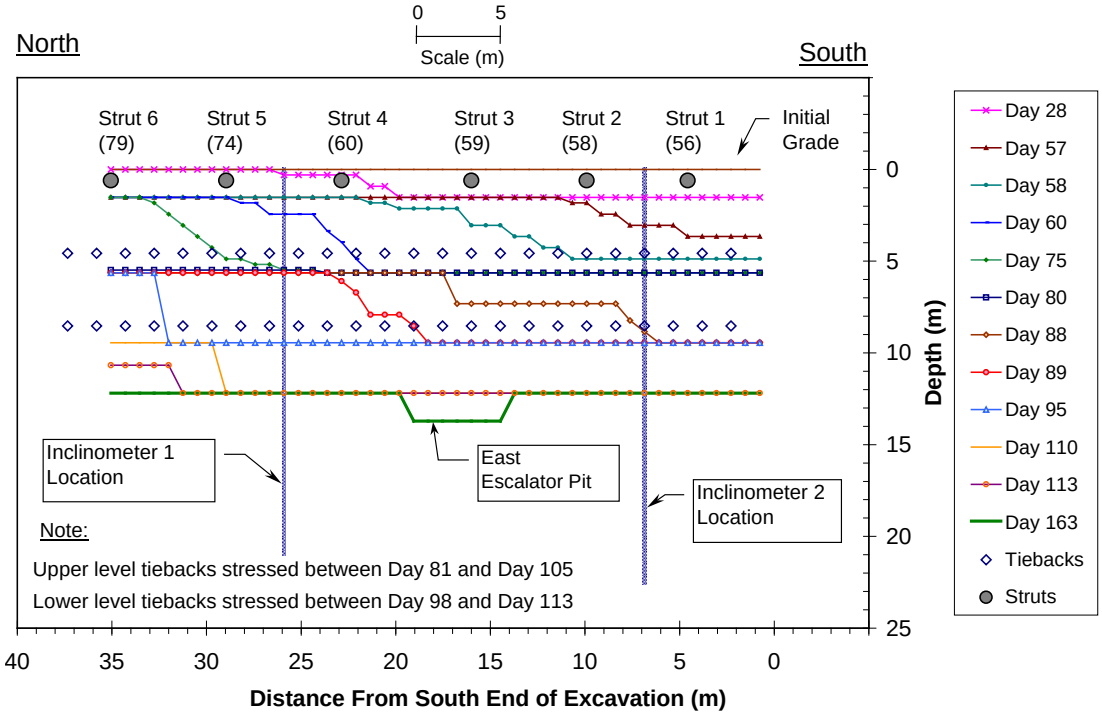

Figure 2: Construction progress at excavation in Chicago (Finno et al 2002).

Even when a sufficiently extensive horizontal excavated surface is identified, 3-dimensional effects may still arise from the higher stiffness at the corners of an excavation. These boundary conditions lead to smaller ground movements near the corners and larger ground movements towards the middle of the excavation wall. Another, and less recognized, consequence of the corner stiffening effects is the maximum movement near the center of an excavation wall may not correspond to that found from a conventional plane strain simulation of the excavation, i.e., 3-dimensional (3-D) and plane strain simulations of the excavation do not yield the same movement at the center portion of the excavation, even if the movements in the center are perpendicular to the wall (Ou et al. 1996). Finno et al. (2007) quantified this effect by the plane strain ratio, PSR, defined as the maximum movement in the center of an excavation wall computed by 3-D analyses divided by that computed by a plane strain simulation. A key indicator is the L/H_e ratio, where L is the dimension of the excavation where the movement occurs, and H_e is the excavation depth. When L/H_e is greater than 6, the PSR is equal to 1 and results of plane strain simulations yield the same displacements in the center of an excavation as those computed by a 3-D simulation. When L/H_e is less than 6, the displacement computed from the results of a plane strain analysis will be larger than that from a 3-D analysis. When conducting an inverse analysis of an excavation with a plane strain simulation, the effects of this corner stiffening is that an optimized stiffness parameter will be larger than it really is because of the lack of the corner stiffening in the plane strain analysis. This effect becomes greater as an excavation is deepened because the L/H_e value increases as the excavated grade is lowered. This trend was observed in the optimized parameters for the deeper strata at the Chicago-State subway renovation excavation (Finno and Calvello 2005).

2.2. Soil Constitutive Behavior: When one undertakes a numerical simulation of a deep supported excavation, one of the key decisions made early in the process is the selection of the material constitutive models representing the various soil formations at the site. If the results form the basis of a prediction that will be

updated based on field performance data, then the types of field data that form the basis of the comparison will impact the applicability of a particular model. Possibilities include lateral movements based on inclinometers, vertical movements at various depths and distances from an excavation wall and/or forces in structural support elements. When used for a case where control of ground movements is a key design consideration, the constitutive model must be able to reproduce the soil response at appropriate strain levels to the imposed loadings.

It is useful to recognize that soil is an incrementally nonlinear material, i.e., its stiffness depends on loading direction and strain level. Soils are neither linear elastic nor elasto-plastic, but exhibit complex behavior characterized by zones of high constant stiffness at very small strains, followed by decreasing stiffness with increasing strain. This behavior under static loading initially was realized through back-analysis of foundation and excavation movements in the United Kingdom (Burland, 1989). The recognition of zones of high initial stiffness under typical field conditions was followed by efforts to measure this ubiquitous behavior in the laboratory for various types of soil (Jardine et al, 1984; Clayton and Heymann 2001; Santagata et al. 2005; Callisto and Calebresi 1998, Holman 2005, Cho 2007). Furthermore, the stiffness depends on the direction of loading, as measured from the most recently applied stress path, or recent stress history.

To illustrate the recent stress history effects on shear stiffness for Chicago clays, secant shear modulus from drained constant mean normal stress (CMS) and constant mean normal stress extension (CMSE) stress paths are plotted versus shear strains in Figure 3. These specimens with an OCR of 1.7 were obtained from block samples cut from an excavation in Evanston, IL (Blackburn and Finno 2007). The angles noted next to the stress paths are calculated as an angle change from the previous stress path ($\theta = 0°$) without consideration of rotation direction. The results of the two "K_0" probe tests showed dependence on the angle change, with the CMSE path (unloading) exhibiting a stiffer response than that of the CME (loading type).

For the "post-unloading" probe tests, with a recent stress history representative of a site where an old building with a basement was demolished before excavation, the opposite directional dependency is observed. The stiffness of loading path (U-CMS) is much greater than those of unloading path (U-CMSE). Interestingly, shear moduli magnitudes in the loading path (K_0-CMS) of the "K_0" probes and the unloading path (U-CMSE) of the "post-unloading" probes with similar values of θ are quite alike, even though the current stress path direction is exactly the opposite. Considering the change in θ, as shown in the inset of Figure 5, the stiffer shear moduli occur at the stress path corresponding to nearly complete stress reversals, U-CMS (θ =160°) and K_0-CMSE (θ =147°). Although the data are limited, it shows the effects of recent stress history on the shear stiffness. Also, little difference was noted at strains larger than 0.1%, as reported by Atkinson (1990) and Atkinson et al (1990). Thus is appears that recent stress history effects are significant for these clays – G_{sec} at about 0.002% strain varies by a factor of 2. Complete details and results of the testing program are presented by Cho (2007).

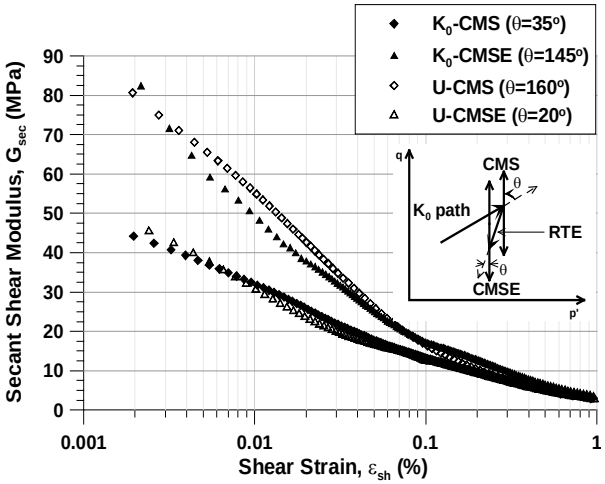

Figure 3: Recent stress history effects on secant shear modulus: Chicago glacial clay.

Burland (1989) suggested that working strain levels in soil around well-designed tunnels and foundations were on the order of 0.1 %. This was also reported by Hashash (1992) for deep excavations. If one uses data collected with conventional triaxial equipment to discern the soil responses, one can reliably measure strains 0.1% or higher. Thus in many practical situations, it is not possible to accurately incorporate site-specific small strain non-linearity into a constitutive model based on conventionally-derived laboratory data.

There are a number of models reported in literature wherein the variation of small strain nonlinearity can be represented, for example, a three-surface kinematic model develop for stiff London clay (Stallebrass and Taylor 1997), MIT-E3 (Whittle and Kavvadas 1994), hypoplasticity models (e.g. Viggiani and Tamagnini 1999), and a directional stiffness model (Tu 2007). These models require either detailed experimental results or experience with the model in a given geology to derive parameters. Alternatively, one can use a neural network based constitutive model wherein the constitutive response is learned based on observed field and laboratory data. Such an approach is embodied in the SELF-SIM method described later in this paper.

For most current practical applications, one uses simpler, elasto-plastic models contained in material libraries in commercial codes. For these models, a key decision is to select the elastic parameters that are representative of the secant values that correspond to the predominant strain levels in the soil mass. Examples of the strain levels behind a wall for an excavation with lateral wall movements of 29 and, 57 mm are shown in Figure 4. These strain levels were computed based on the results of displacement-controlled simulations where the lateral wall movements and surface settlements were incrementally applied to the boundaries of a finite element mesh. The patterns of movements were typical of excavations through clays, and were based on those observed at an excavation made through Chicago clays (Finno and Blackburn 2005). Because the simulations were displacement-controlled, the computed strains do not depend on the assumed constitutive behavior.

As can be seen in Figure 4, the maximum shear strains correspond to about 0.3% for 29 mm maximum wall lateral movement, and represent good control of ground movements in these soft soils. Shear strains as high as 0.7% occurred when 57 mm of maximum wall movement develop. These strain levels can be accurately measured in conventional triaxial testing, and thus if one can obtain specimens of sufficiently high quality, then secant moduli corresponding to these strain levels can be determined via conventional laboratory testing. Because the maximum horizontal wall displacement can be thought of as a summation of the horizontal strains behind a wall, the maximum wall movements can be accurately calculated with a selection of elastic parameters that correspond to these expected strain levels. In Figures 4a and 4b, the fact that small strain non-linearity is not explicitly considered will not have a large impact on the computed horizontal wall displacements because they are dominated by the larger strains in the soil mass. Consequently, these computed movements would be compatible with those measured by an inclinometer located close to the wall.

However, if one needs to have an accurate representation of the distribution of ground movements with distance from the wall, then this approach of selecting strain-level appropriate elastic parameters will not work. The small strain non-linearity must be explicitly considered to find the extent of the settlement because the strains in the area of interest vary from the maximum value to zero. As a consequence, many cases reported in literature indicate computed wall movements agree reasonably well with observed values, but the results from the same computations do not accurately reflect the distribution of settlements. Good agreement at distances away from a wall can be obtained only if the small stain non-linearity of the soil is adequately represented in the constitutive model.

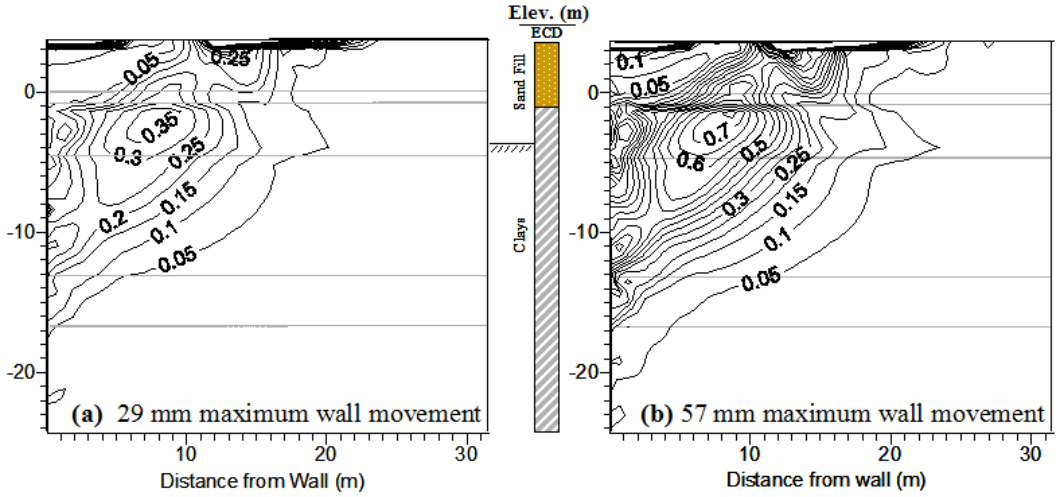

Figure 4: Shear strain levels behind excavation (contours in %).

3. Monitoring Data: The assumptions inherent in any prediction limit the types of data that can be used as a basis of updating performance predictions. Consequently, one must carefully select the types of data, location of the measuring points, and the excavation conditions when applying an inverse technique. Inclinometer data based on measurements close to a support wall are the most useful when typical elasto-plastic constitutive models are assumed to represent soil behavior, as is the case when employing commercial finite element codes, for reasons discussed in the last section. These data can be supplemented by ground surface settlements when using a constitutive model that accounts for small strain nonlinearities and dilation (Finno and Tu 2006, Hashash and Whittle, 1996). Furthermore, other types of measurements, such

as forces in internal braces and pore water pressures, conceptually can be used in conjunction with displacement measurements to make the computed results more sensitive to parameters selected for optimization (Rechea 2006).

While these different types of data can be handled within a properly formulated inverse analysis, the timely collection and screening of the data must be successfully accomplished. Furthermore, for any monitoring system to be fully automated, one must be able to track construction progress so that performance data can be correlated with the excavation activities. To correlate the numerical data with the causative actions of the excavation process, imaging technologies can be employed to provide an accurate and detailed record of construction activities. Three-dimensional laser scanning is a relatively new technology that utilizes LIDAR (Light Detection and Ranging). Trupp et al. (2004) and Su et a. (2006) used 3-D laser scanning to capture an accurate image of the geometry of the excavation to provide an accurate, as-built digital record of construction. Sections may be taken from these scans and imported into a finite element code to provide an accurate excavation surface for input to inverse analysis. An internet accessible weather-resistant video camera has been used on several projects to allow remote visualization of the construction process in real-time, as well as a dated, photographic record of construction (Finno and Blackburn 2005). Significant developments have been made in automated wireless systems to continuously monitor deformations due to construction activities. These systems provide the engineer with uninterrupted stream of data in near real time without the need to wait for manual data readings. Such systems are essential tools for making timely decisions regarding changes in construction activities and support installation to mitigate potential damage to adjacent facilities. A number of these and examples of their use are included in the following sections.

3.1. Laser Scanning: Three-dimensional laser scanning is a relatively new technology that utilizes LIDAR (Light Detection and Ranging). It is similar to RADAR (Radio Detection and Ranging), but uses light to measure range or distance. A laser scanner consists of an emitting diode that produces a light source at a very specific frequency. A mirror directs the laser beam (with a diameter of 6 mm) horizontally and vertically towards the target. The surface of the target then reflects the laser beam. Using the principles of pulse time of flight the distance can be determined by the transit time, with a precision of +/- 6 mm. The result of a scan produces point clouds and is processed into accurate 3D models.

The practical use of laser scanning was demonstrated at the Northwestern University Ford Motor Company Engineering Design Center excavation (Trupp et. al. 2004). With an approximate dimension of 36 m x 45 m (length x width), an excavation supported by an internally-braced sheet pile wall was made between mid-January and mid-May, 2004. During this entire period a laser scanner was employed weekly to carry out the 3-D field scanning. It represents the first use of 3-D laser scanning on a routine basis at an open excavation site. The scans provide 3-D to scale geometric dimensions of the excavation as illustrated in Figure 5. One must acquire accurate records of construction staging in deep excavations to understand and predict the field responses to excavation as well as impacts on nearby facilities. The terrain model can be automatically imported into a numerical simulation environment to improve the fidelity of model simulation. This information can be used for construction management functions as well and to develop as-built drawings of unprecedented accuracy.

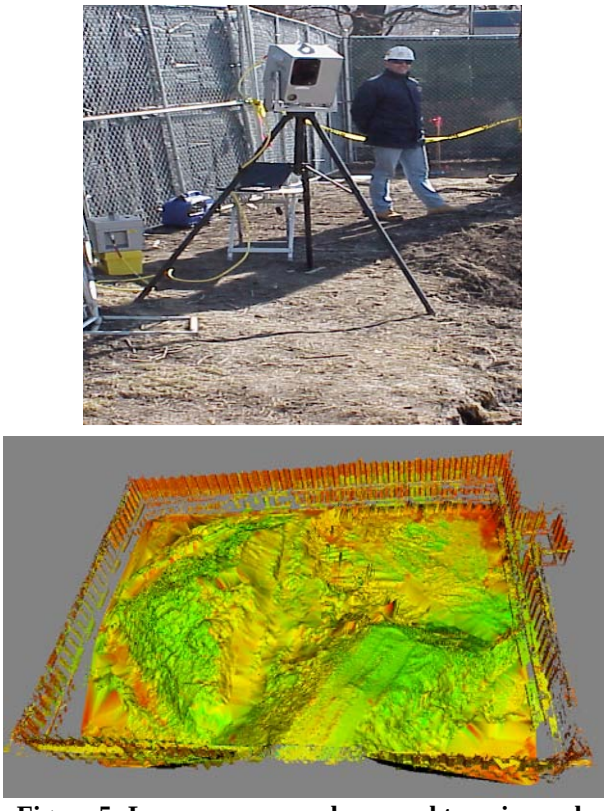

Figure 5: Laser scanner and scanned terrain mesh for Ford Center Excavation.

3.2. Webcams: The authors have used an internet accessible weather-resistant video camera (“webcam”) on several projects to monitor the construction process in real-time as illustrated in Figure 6. Webcams can be installed with features that allow a password restricted

user to pan and zoom to allow details of the construction to be observed. The images can be made accessible via a website to the general public, including project engineers, contractors and owners. The images also can be combined with the automated survey and tiltmeter data to observe the response to the excavation process in real-time from a remote location and to relate it qualitatively to construction operations. Laser scan images can be used to relate such data quantitatively, as described by Quiñones-Rozo et al. (2008).

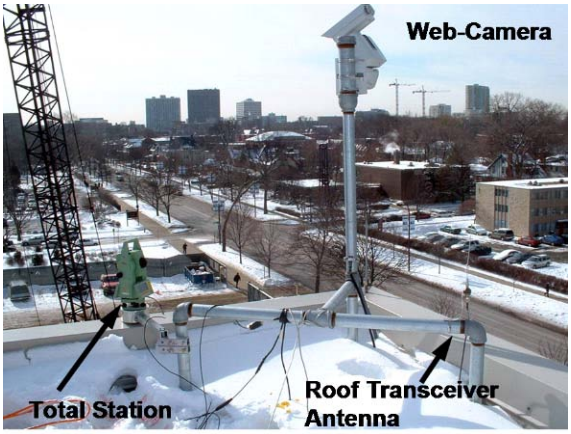

Figure 6: Total Station and webcam on rooftop of adjacent building.

3.3. Automated Total Surveying Station: The authors have employed a total surveying station to monitor the displacement of optical prisms placed at various locations around an excavation site. The total station is shown in figure 6 mounted via an aluminum mounting plate and swing-arm apparatus on the roof of an adjacent building. The total station was configured to allow communication via RS232 data transmission to a transceiver such that radio communication was established between the total station and a remote host computer. All point position data are calculated relative to at least two fixed reference points which allows for slight instrument movement during operation and allows the instrument to be removed for repairs, if necessary. Also, by calculating the positions of the reference points relative to each other, instrument tilt can be detected. Accuracy of the system was computed to be ± 2.8 mm.

Optical surveying prisms were installed at selected locations to monitor the deformation of adjacent soil and structures during the excavation process. The automated acquisition of the data allow it to be imported directly into a self-updating numerical model in real time so that updated predictions of performance can be made in a timely fashion. In contrast to conventional survey data which can take 1 to 2 weeks to find its way to a decision maker, this system allows one to evaluate it immediately. Figure 7 shows typical horizontal movement data obtained in real time from an automated total station from the Ford Center excavation.

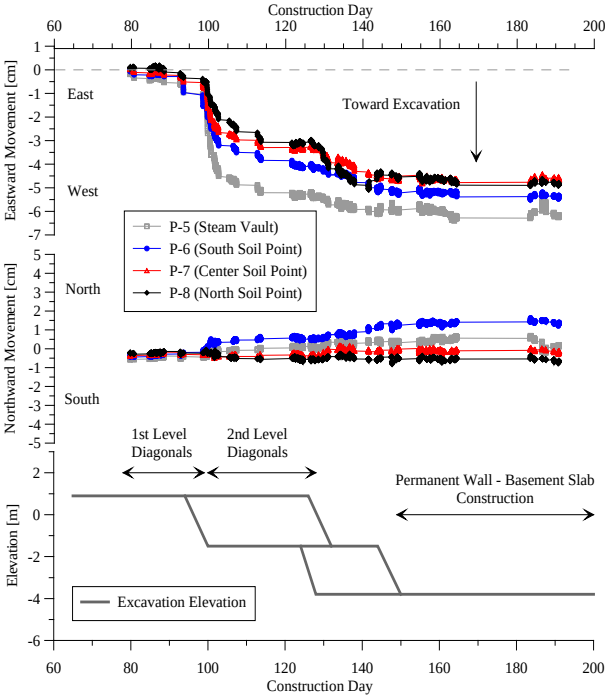

Figure 7: Typical movement at Ford Center excavation from automated total station.

3.4. Remote Access Tiltmeters: Tilt is important because it allows one to compute the angular distortion – a parameter that is correlated with observed damage – if the settlement distribution is known. We have employed remote access tiltmeters on selected structural elements of the building affected by excavation activities to monitor the response of the structure during excavation. The tiltmeters were attached to columns and walls with a quick-setting epoxy and coupled with Freewave point-to-point radio transceivers to allow continuous remote data collection.

Correlating tilt measurements to ground movements allows the structural response of an affected building to the excavation activities to be directly evaluated when coupled with structural models (e.g. Finno et al. 2005). After all, it is protection of the adjacent structures that is the design objection in many excavations in congested urban areas.

4. Inverse Analysis: In model calibration, various parts of the model are changed so that the measured values are matched by equivalent computed values until the resulting calibrated model accurately represents the main aspects of the actual system. In practice, numerical models typically are calibrated using trial-and-error methods. Inverse analysis works in the same way as a non-automated calibration approach:

parameter values and other aspects of the model are adjusted until the model's computed results match the observed behavior of the system.

Inverse analysis techniques have been applied to geotechnical problems since the 1980s (e.g., Gioda and Maier 1980; Sakurai and Takeuchi 1983). Its use allows one to evaluate performance of geotechnical structures by a quantifiable observational method. It has been used to identify soil parameters from laboratory or in situ tests (e.g., Anandarajah and Agarwal 1991), and performance data from excavation support systems (e.g., Ou and Tang1994; Calvello and Finno 2004; Finno and Calvello 2005; Levasseur et al. 2007), excavation of tunnels in rock (Sakurai and Takeuchi, 1983; Gens et al. 1996) and embankment construction on soft soils (Arai et al., 1986; Wakita and Matsuo, 1994). Many of the previous evaluations of performance data were conducted with very simple soil models that severely restricted the ability of the computations to accurately reflect the observed field performance data, irrespective of employing inverse techniques.

Use of an inverse model provides results and statistics that offer numerous advantages in model analysis and, in many instances, expedites the process of adjusting parameter values. The fundamental benefit of inverse modeling is its ability to calculate automatically parameter values that produce the best fit between observed and computed results. The main difficulties inherent to inverse modeling algorithms are complexity, non-uniqueness, and instability. Complexity of real, non-linear systems sometimes leads to problems of insensitivity when the observations do not contain enough information to support estimation of the parameters. Non-uniqueness may result when different combinations of parameter values match the observations equally well. Instability can occur when slight changes in model variables radically change inverse model results. Although these potential difficulties make inverse models imperfect tools, work in related civil engineering fields (e.g., Poeter and Hill, 1997) demonstrate that inverse modeling provides capabilities that help modelers significantly, even when the simulated systems are very complex.

Two main types of inverse analysis have been applied to geotechnics, optimization by iterative algorithms such as gradient methods (e.g., Ou and Tang 1994; Ledesma et al., 1996; Calvello and Finno 2004) and optimization by techniques from the field of artificial intelligence, including artificial neural networks (Yamagami et al. 1997; Hashash et al. 2006) and genetic algorithms (Levasseur et al. 2007). The gradient method employs a local parameter identification of a specific constitutive law. The artificial neural network is a method which creates by learning phases its own constitutive law from geotechnical measurements. Genetic algorithms are global optimization methods which localize an optimum set of solutions close to the "true" value. Both a gradient method and an artificial neural net approach will be described herein.

4.1. Gradient Method of Inverse Analysis: The gradient method described herein uses UCODE (Poeter and Hill, 1998), a computer code designed to allow inverse modeling posed as a parameter estimation problem. Macros can be written in a windows environment to couple UCODE with any application software.

Figure 8 shows a flowchart of the parameter optimization algorithm used in UCODE. With the results of a finite element prediction in hand, the computed results are compared with field observations in terms of weighted least-squares objective function, S(b):

$$S(\underline{b}) = \left[\underline{y} - \underline{y}'(\underline{b})\right]^T \underline{\omega}\left[\underline{y} - \underline{y}'(\underline{b})\right] = \underline{e}^T \underline{\omega e} \quad (1)$$

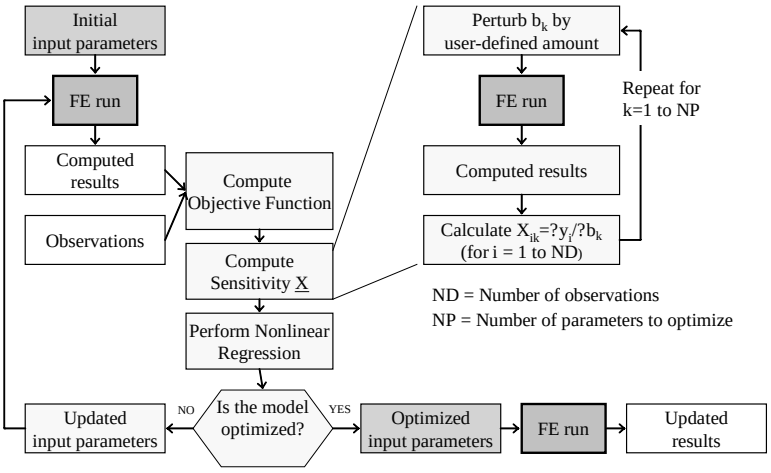

Figure 8: Flow chart for inverse analysis.

where $\underline{b}$ is a vector containing values of the parameters to be estimated; $\underline{y}$ is the vector of the observations being matched by the regression; $\underline{y'(b)}$ is the vector of the computed values which correspond to observations; $\underline{\omega}$ is the weight matrix wherein the weight of every observation is taken as the inverse of its error variance; and $\underline{e}$ is the vector of residuals. This function represents a quantitative measure of the accuracy of the predictions.

A sensitivity matrix, $\underline{X}$, is then computed using a forward difference approximation based on the changes in the computed solution due to slight perturbations of the estimated parameter values. This step requires multiple runs of the finite element code. Regression analysis of this non-linear problem is used to find the values of the parameters that result in a best fit between the computed and observed values. In UCODE, this fitting is accomplished with the modified Gauss-Newton method, the results of which allow the parameters to be updated using:

$$\left(\underline{C}^T \underline{X}_r^T \omega \underline{X}_r \underline{C} + \underline{I}\, m_r\right)\underline{C}^{-1}\underline{d}_r = \underline{C}^T \underline{X}_r^T \omega\left(\underline{y} - \underline{y}'(\underline{b}_r)\right) \quad (2)$$

$$\underline{b}_{r+1} = \rho_r \underline{d}_r + \underline{b}_r \quad (3)$$

where d_r is the vector used to update the parameter estimates b; r is the parameter estimation iteration number; X_r is the sensitivity matrix ($X_{ij}=\partial y_i/\partial b_j$) evaluated at parameter estimate $\underline{b}_r$; $\underline{C}$ is a diagonal scaling matrix with elements c_{jj} equal to $1/\sqrt{(\underline{X}^T \underline{\omega}\, \underline{X})_{jj}}$; $\underline{I}$ is the identity matrix; m_r is the Marquardt parameter used to improve regression performance; and $\underline{d}_r$ is a damping parameter, computed as the change in consecutive estimates of a parameter normalized by its initial value, but is restricted to values less than 0.5.

At a given iteration, after performing the modified Gauss-Newton optimization, the updated model is considered optimized if either of two convergence criteria is met: (i) the maximum parameter change of a given iteration is less than a user-defined percentage of the value of the parameter at the previous iteration; (ii) the objective function, S($\underline{b}$), changes less than a user-defined amount for three consecutive iterations.

After the model is optimized, the final set of input parameters is used to run the finite element model one last time and produce the "updated" prediction of future performance. See Rechea (2006) for details concerning the convergence criteria as applied to excavations.

4.1.1. Weighting Function: The weight of an observation can be expressed as the inverse of the variance for the 95% confidence interval for the accuracy of a measurement:

$$weight = \frac{1}{\sigma^2} \qquad \sigma = \frac{Accuracy}{1.96} \quad (4)$$

In this way, more reliable data (smaller variability) are given greater emphasis, or weight. The errors associated to measurements are usually related to the accuracy of the instrumentation, and independent of the magnitude of the observation (assuming the observation is within the range of the instrumentation). Table 1 shows how to obtain weights for various types of instrumentation. Accuracies and ranges in Table 1 are taken from manufacturer's literature, and are meant to be representative of typical values in the field. Smaller values can be used based on field data collected prior to any activity at the site, assuming enough data are collected to adequately define the variation about the initial value (Langousis 2007).

4.1.2. Selection of Parameters: The relative importance of the input parameters being simultaneously estimated can be defined using various parameter statistics (Hill 1998). The statistics found useful for this type of work are the composite scaled sensitivity, ccs_j, and the correlation coefficient, $cor(i,j)$. The value of css_j indicates the total amount of information provided by the observations for the estimation of parameter j, and is defined as:

$$css_j = \left[\sum_{j=1}^{ND}\left(\left(\frac{\partial y'_i}{\partial b_j}\right) b_j \omega_{ii}^{1/2}\right)^2 \Bigg|_{\underline{b}} \Big/ ND\right]^{1/2} \quad (5)$$

where y'_i is the i^{th} computed value, b_j is the j^{th} estimated parameter, $\partial y_i/\partial b_j$ is the sensitivity of the i^{th} computed value with respect to the j^{th} parameter, ω_{jj} is the weight of the i^{th} observation, and ND is the number of observations.

The values of the matrix $cor\ (i,j)$ indicate the correlation between the i^{th} and j^{th} parameters, and are defined as:

$$cor(i,j) = \frac{\mathrm{cov}(i,j)}{\mathrm{var}(i)^{1/2}\,\mathrm{var}(j)^{1/2}} \quad (6)$$

where cov(i,j) equal the off-diagonal elements of the variance-covariance matrix $\underline{V}(\underline{b}')=s^2(\underline{X}^T\underline{\omega}\underline{X})^{-1}$, and var($i$) and var($j$) refer to the diagonal elements of $\underline{V}(\underline{b}')$.

Inverse analysis algorithms allow the simultaneous calibration of multiple input parameters. However, identifying the important parameters to include in the inverse analysis can be problematic, and it is not possible to use a regression analysis to estimate every input parameter of a given excavation simulation. The number and type of input parameters that one can expect to estimate simultaneously depend on a number of factors, including the soil models used, the stress conditions of the simulated system, available observations, and numerical implementation issues. Examples of this procedure are presented by Calvello and Finno (2004) and Finno and Calvello (2005).

Table 1: Typical weights of observations

Instrumentation	Range (full scale)	Accuracy	95% standard deviation, σ	Weight
Lateral movements with inclinometers	± 53° from vertical	± 0.25 mm/m $\frac{0.25}{1000}\cdot d$	$\frac{0.25}{1000}\cdot\frac{d}{1.96}=0.0001\cdot d$ (m)	$\frac{1}{(0.0001\cdot d)^2}$
		where *d* is distance (m) from bottom of casing		
Ground surface settlement with optical survey		± 0.01 ft ± 0.003 m	$\frac{0.003}{1.96}=0.00155$ (m)	$\frac{1}{(0.00155)^2}$
vibrating wire piezometer	3.5 bar/50 psi 344.8 Pa	± 0.1% FS ± 0.34 Pa	$\frac{0.34}{1.96}=0.173$ (Pa)	$\frac{1}{(0.173)^2}$
Strut force with spot-weldable strain gauge	2,500 microstrain	± 0.1%FS = ± 2.5 microstrain	$\frac{E\cdot A\cdot Accuracy}{1.96}$ (kN)	$\frac{1}{(6.19)^2}$ (1)

(1) value shown is for a steel brace with A = 0.024 m^2

4.1.3. Examples of the Gradient Method: Several examples of the gradient method applied to supported excavations are presented to illustrate (i) its ability to identify optimized parameters based on observations made during early stages of excavation so as to allow accurate predictions of performance of latter stages of an excavation, and, (ii) the applicability of optimized parameters found based on performance data of one excavation to others in the same geology.

The finite element software PLAXIS was used to compute the plane strain response of the soil around these excavations. The inverse techniques contained in UCODE can be coupled with any application software, and it also has been successfully coupled with ABAQUS and other research-oriented finite element codes. For purposes of brevity, only PLAXIS applications with the hardening-soil model (H-S) (Schanz et al. 1999) are presented in this paper. Parameters from other constitutive models have been optimized as well (e.g., Calvello and Finno 2002).

The effective stress H-S model is formulated within the framework of elasto-plasticity. Plastic strains are calculated assuming multi-surface yield criteria. Isotropic hardening is assumed for both shear and volumetric strains. The flow rule is non-associative for frictional shear hardening and associative for the volumetric cap. Six basic H-S input parameters define the constitutive soil responses, the friction angle, φ, cohesion, c, dilation angle, ψ, the reference secant Young's modulus at the 50% stress level, E_{50}^{ref}, the reference oedometer tangent modulus, E_{oed}^{ref}, and the exponent *m* which relates reference moduli to the stress level dependent moduli (E representing E_{50}, E_{oed}, and E_{ur}):

$$E = E^{ref}\left(\frac{c\cot\phi - \sigma_3^{'}}{c\cot\phi + p^{ref}}\right)^m \quad (7)$$

where p^{ref} is a reference pressure equal to 100 stress units and σ'_3 is the minor principal effective stress. A sensitivity analysis indicated that the model's relevant and uncorrelated parameters for the Chicago excavations presented herein are E_{50}^{ref} and φ' (Calvello and Finno 2004). Results were also sensitive to changes in values of parameter *m*. However, parameter *m* was not included in the regression because the values of the correlation coefficients between parameters *m* and E_{50}^{ref} were very close to 1.0 at every layer, indicating that the two parameters were not likely to be simultaneously and uniquely optimized. When values of φ' were kept constant at their initial estimates, and only the stiffness parameters, E_{50}^{ref}, were optimized, the calibration of the simulations presented subsequently was successful. Finno and Calvello (2005) showed that shear stress levels in the soil around the excavation were much less than those corresponding to failure for the great majority of the soil. This is indeed expected for excavation support systems that are designed to restrict adjacent ground movements to acceptably small levels, and hence one would expect the stiffness parameters to have a greater effect on the simulated results than failure parameters.

4.1.3.1. Parameter Optimization at Early Stages of Excavation: The ability of the approach to provide optimized parameters at an early stage of excavation which leads to good predictions of subsequent performance is illustrated by the Chicago Ave. and State St. subway renovation project in Chicago (Finno et al. 2002). This project involved the excavation of 12.2 m of soft to medium clay within 2 m of a school supported on shallow foundations. Figure 9 shows a section of the excavation support system. The support system consisted of a secant pile wall with three levels of support, which included pipe struts (1st level) and tieback anchors (2nd and 3rd levels).

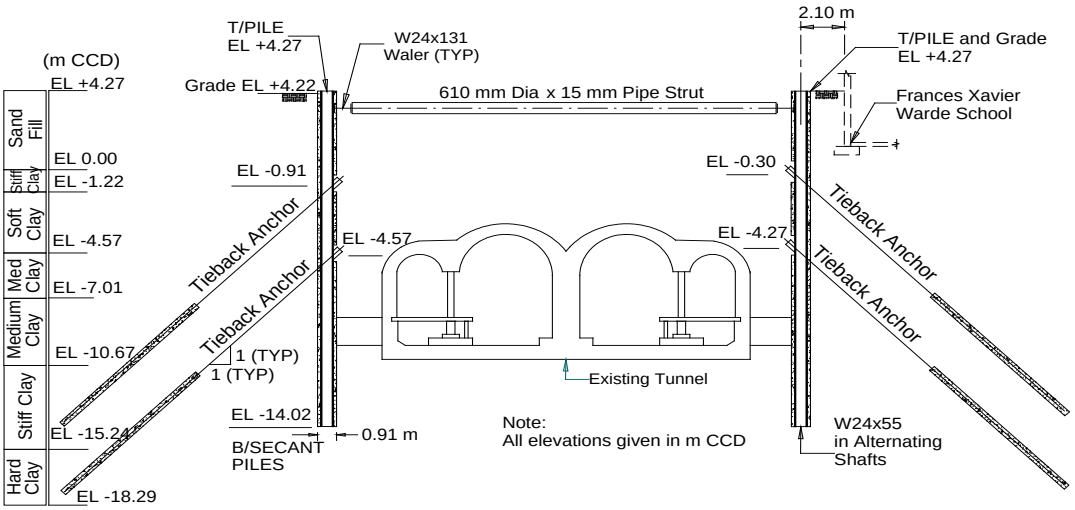

Figure 9: Support system for Chicago-State excavation (Finno et al. 2002).

The subsurface conditions consisted of an urban fill, mostly medium dense sand but also containing construction debris, overlying four strata associated with the repetitive process of advance and retreat of the Wisconsin glacier. The upper three are ice margin deposits deposited underwater, and are distinguished by water content and undrained shear strength (Chung and Finno, 1992). With the exception of a clay crust in the upper layer, these deposits are lightly overconsolidated as a result of lowered groundwater levels after deposition and/or aging. Stratigraphy is shown in terms of Chicago City Datum (CCD) elevation.

A complete record of performance of the excavation can be found in Finno et al. (2005). Figure 10 summarizes deformation responses to excavation and support. Both lateral movements and settlements are shown. The movements that occurred as the secant pile wall extend through all compressible layers. This is important when using these observations to calibrate parameters using inverse techniques in that these movements occur at an early stage of the excavation, and hence contain information that can be used to optimize parameters in all layers that can be useful to predict movements at subsequent stages of excavation.

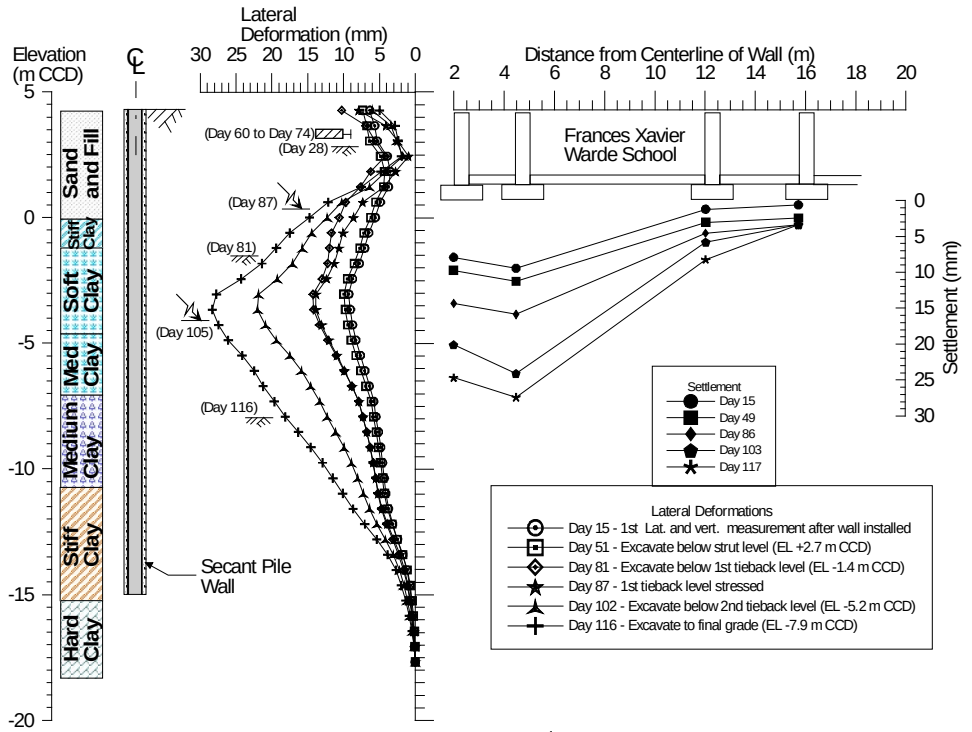

Figure 10: Lateral movements and settlements at Chicago-State excavation (Finno et al. 2002).

Very little movement beyond that which occurred during wall installation were observed until the excavation was lowered below EL. –1.4 m CCD; a maximum of 4 mm additional lateral movement occurred as a result of excavating to this elevation. This behavior suggests that the upper clays initially are relatively stiff, and provide field indications of the small strain nonlinearity of these soils. After wall installation, the secant pile wall incrementally moved toward the excavation in response to excavation-induced stress relief. When the excavation reached final grade, the maximum lateral movement was 28 mm. The school settled as the secant pile wall moved laterally. The maximum settlement at the school at the end of excavation was also 28 mm.

Table 2 shows the calculation phases and the construction stages used in the finite element simulations. Note that the tunnel tubes and the school adjacent to the excavation were explicitly modeled in the first 12 phases of the simulation to take into account the effect of their construction on the soil surrounding the excavation. Stages 1, 2, 3, 4 and 5 in the optimization process refer to the construction stages for which the computed results were compared to inclinometer data taken from two inclinometers on opposite sides of the excavation. Construction steps not noted as "consolidation" on Table 2 were modeled as undrained. Consolidation stages were included after the tunnel, school and wall installation calculation phases to permit excess pore water pressures to equilibrate. To simulate secant pile wall installation in the plane strain analysis, elements representing the wall were excavated and a hydrostatic pressure equivalent to a water level located at the ground surface was applied to the face of the resulting trench (calculation phase 13 in Table 2). After computing the movements associated with this process, the excavated elements were replaced by elements with the properties of the secant pile wall (calculation phase 14). Details about the definition of the finite element problem, the calculation phases and the model parameters used in the simulation can be found in Calvello (2002).

Visual examination of the horizontal displacement distributions at the inclinometer locations provides the simplest way to evaluate the fit between computed and measured field response. When computations were made based on parameters derived from results of drained triaxial tests, the finite element model computed significantly larger displacements at every construction stage (Finno and Calvello 2005). The maximum computed horizontal displacements are about two times the measured ones and the computed displacement profiles result in significant and unrealistic movements in the lower clay layers. As one would expect, these results indicated that the stiffness properties for the clay layers based on conventional laboratory data were less than field values.

Table 2: FE simulation of construction.

Phase	Construction step	Simulation stage
0	Initial conditions	
1-4 5	Tunnel construction (1940) Consolidation	
6-10 11-12	School construction (1960) Consolidation	
13	Drill secant pile wall (1999)	
14	Place concrete in wall	Stage 1
15	Consolidation (20 days)	
16	Excavate and install struts	Stage 2
17	Excavate below first tieback level	
18	Prestress first level of tiebacks	Stage 3
19	Excavate below second tieback level	
20	Prestress second level of tiebacks	Stage 4
21	Excavate to final grade	Stage 5

Figure 11 shows the comparison between the measured field data from both sides of the excavation and the computed horizontal displacements when parameters are optimized based on stage 1 observations. The improvement of the fit between the computed and measured response is significant. Despite the fact that the optimized set of parameters is calculated using only stage 1 observations, the positive influence on the calculated response is substantial for all construction stages. At the end of the construction (i.e. stage 5) the maximum computed displacement exceeds the measured data by only about 15%. These results are significant in that a successful recalibration of the model at an early construction stage positively affects subsequent "predictions" of the soil behavior throughout construction.

Analyses were also made wherein parameters were recalibrated at every stage until the final construction stage (stage 5). At every new construction stage, the inclinometer data relative to that stage were added to the observations already available. Results indicated that difference between the fit shown in Figure 11 and with those calibrated after every increment was not significant. In essence, the inverse analysis performed after the first construction stage "recalibrated" the model parameters in such a way that the main behavior of the soil layers could be accurately predicted throughout construction.

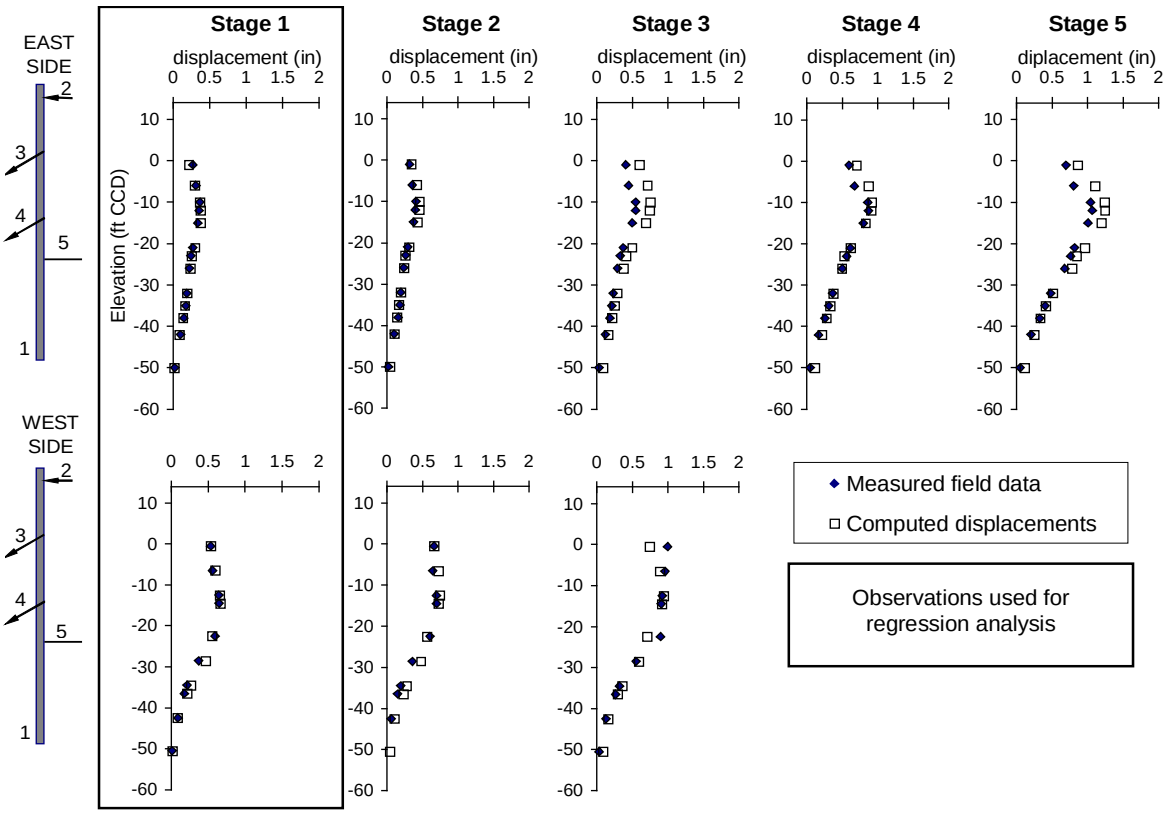

Figure 11: Comparison of observed and computed horizontal displacements (after Finno and Calvello 2005).

4.1.3.2. Applicability of Optimized Parameters at Other Locations in Same Deposit: To show the applicability of the optimized parameters that formed the basis of the good agreement in Figure 11 to other excavation sites in these soil deposits, the results of numerical simulations are presented in Figure 12 based on these optimized parameters for the Lurie (Finno and Roboski 2005) and the Ford Design Center (Blackburn and Finno 2007) excavations. The geologic origin of the most compressible material is similar for all three cases, but the Lurie Center is located about 2 km from the Chicago-State site and the Ford Center is located about 15 km from the site. Consequently one should expect some variability in the actual parameters at each site.

Examining the comparisons in the clay layers below EL. –15 ft CCD for the Lurie data, reasonable agreement is observed at stages 4 and 6, with significant differences seen at the intermediate stage 5. While the reasons for this are not entirely clear, the difference between the excavated levels for stages 5 and 6 was only 2 m. The observed lateral movements from stage 5 might have been impacted by the excavation process not being completely uniform. This emphasizes the need to carefully select stages for analysis that are compatible with the assumed numerical model – in this case a plane strain representation of the problem. While care was taken to do so, some simplification of the excavation process was necessary in order to obtain a complete record of the responses. Furthermore, the computed results indicated much larger cantilever type movements than were observed. This difference was due to the representation of the tiebacks in the plane strain simulation (Finno and Tu 2006).

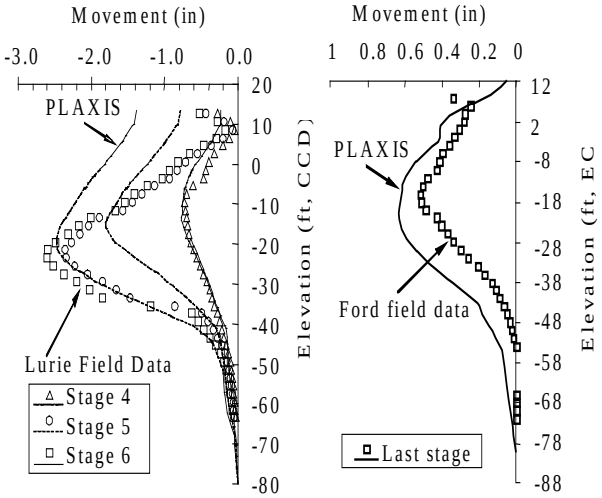

Figure 12: Computed and observed lateral movements based on optimized parameters from Chicago-State excavation.

At the Ford Center, the numerical results shown in Figure 12 followed similar trends as the observed data, but with larger magnitudes. This is likely caused by the fact that the H-S model used herein does not include provisions to represent the large stiffness degradation with small strains. One must select moduli that represent the average strains within the soil mass, and when the movements are small, the average modulus should be higher in a model that does not consider the small strain modulus degradation. The parameters used in the analysis were based on the larger deformations that were present at the Chicago-State site, and hence resulted in larger deformations than were observed at the Ford Center. In any case, the application of the Chicago-State based optimized parameters to both the Lurie and Ford sites resulted in reasonable agreement with the observed lateral movements, within the limitations of the analyses. Application of the inverse techniques to these data resulted in improved fit with minor changes to the parameters (Rechea 2006).

4.2. SelfSim Self Learning Engineering Simulations: A novel inverse analysis method, self-learning in engineering simulations (SelfSim), is introduced to integrate precedence into numerical simulations. SelfSim extracts relevant constitutive soil information directly from field measurements of excavation response such as lateral wall deformations and surface settlement. The resulting soil model, used in a numerical analysis, provides ground deformations consistent with observed behavior of the current excavation and can be used in the prediction of behavior of similar excavations. The soil model can continuously evolve using additional field information. SelfSim framework application to excavation problems is illustrated in Figure 13 (Hashash et al., 2003, Hashash et al., 2005, Hashash et al., 2006). In a typical excavation problem, wall deformations and surface settlements are measured at selected excavation stages (step 1). The measured deformations and the corresponding known excavation stage represent complementary sets of field observations. A numerical model of this excavation problem will have to correctly represent this pair of field observations. A numerical model is developed to simulate the construction sequence. A neural network (NN) based constitutive model is used to simulate the soil response. Initially the soil response is unknown and the NN soil model is pre-trained using stress strain data that reflect linear elastic response over a limited strain range. Additional available soil behavior information, such as that from laboratory tests, can be used in this initialization process.

In step 2a of SelfSim a finite element analysis using the current NN soil model is performed simulating soil removal and support installation corresponding to a given excavation stage. SelfSim stipulates that due to equilibrium considerations and the use of correct boundary forces due to soil removal, the corresponding computed stress field provides an acceptable approximation of the "true" stress field experienced by the soil.

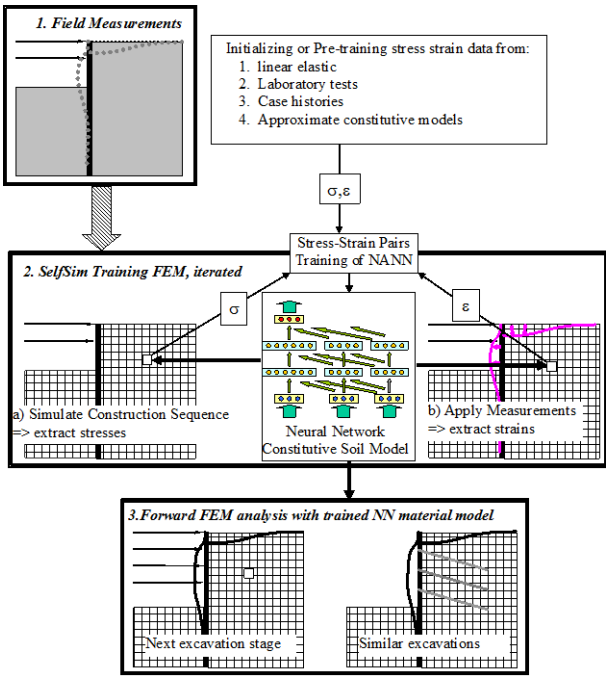

Figure 13: SelfSim learning Training, Lurie Excavation Site.

In step 2b of SelfSim a parallel FE analysis using the same NN soil model is performed in which the lateral wall deflections and surface settlements are imposed as additional displacement boundary conditions. The computed equilibrium strain field provides an acceptable approximation of the "true" strain field experienced by the soil.

The stress field from step 2a and the strain field from step 2b are extracted to form stress-strain pairs that approximate the soil constitutive response and used to re-train the NN soil model. The analyses of step 2 are repeated and the solution converges when the analysis of Step 2a provides the correct ground deformation, i.e. analyses of step 2a and step 2b provide similar results. The resulting, extracted, soil constitutive model can be used in the analysis of other types of excavations in similar ground conditions or a later excavation stage as illustrated in Step 3 of Figure 13. The predictive capability of the model can be extended by a) additional SelfSim training using other available excavation case histories, b) using additional laboratory test data, and c) using conventional constitutive model at stress and strain levels outside those extracted from SelfSim training.

SelfSim is used to learn from observations at the Lurie Research Center excavation in downtown Chicago, IL (Marulanda et al. 2005). The excavation was approximately 82 by 69 m with a depth of approximately 13 m (Finno and Roboski 2004). As shown in Figure 14, the support system consisted of a sheet pile wall with three levels of tiebacks. The site was heavily instrumented to monitor the ground movements resulting from the excavation including lateral deflections and surface settlements. The individual soil formations are represented using separate NN based constitutive models.

Figure 15 shows the learned deformations after ten passes of training using data from all construction stages. Overall, the computed deformations at this stage of training are similar to the field measurements. Most movement occurs within the clay layers when the excavation reaches the excavation level -5.8m and is reflect as an abrupt increase in measured deformation which may reflect the transition from "small" to "large" strain responses of the clay, a common occurrence in Chicago area excavations. There were no intermediate deformation measurements between excavation levels -2.4 m (Stage 4) and -5.8 m (Stage 5) where maximum wall deformations increased from 10 to 60 mm. The lack of intermediate information reduces the opportunity to more accurately learn the clay behavior and increases the difficult of SelfSim learning.

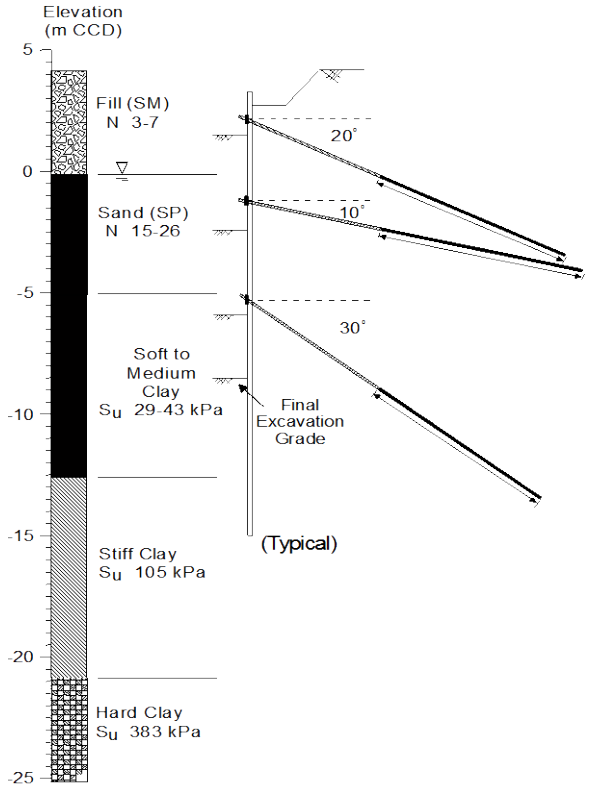

Figure 14: Subsurface conditions and support system at the Lurie Center excavation.

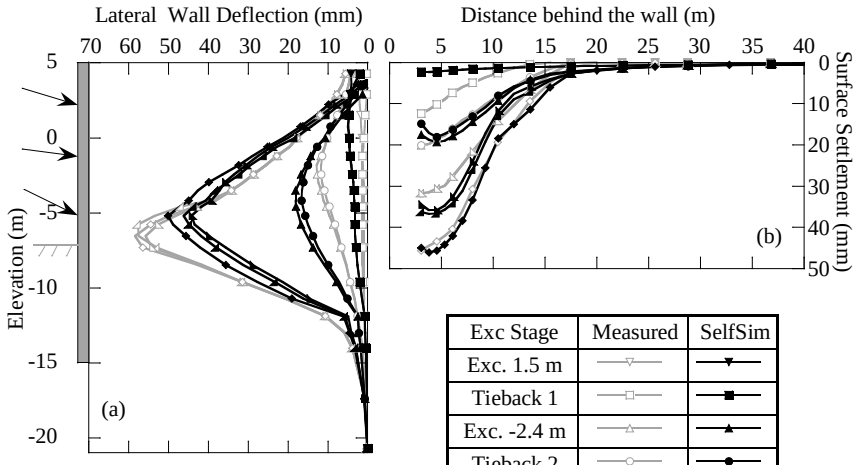

Figure 15: Lateral soil movement and surface settlement after ten passes of SelfSim learning.

The computed soil movements agree very well with the field measurements, though there are some noticeable discrepancies in the initial two stages between the computed and the measured soil movements. The extracted soil model for the soft clay was compared to measured behavior conducted at Northwestern University as shown in Figure 16. The extracted soft clay soil model developed from the SelfSim training gives a reasonable estimate of non-linear response for strains less than 0.5%.

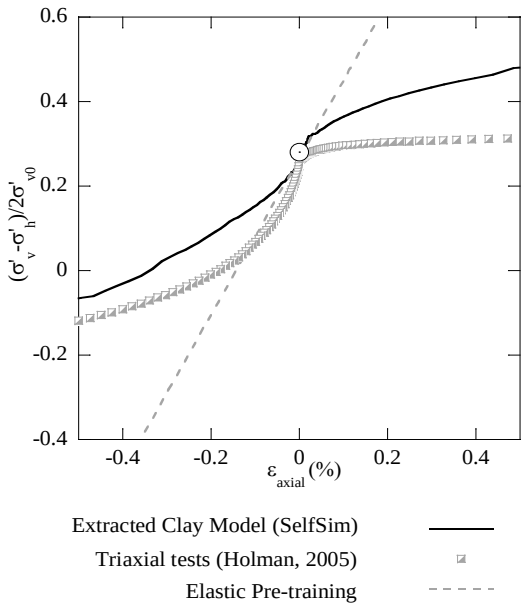

Figure 16: Comparison between triaxial tests performed at Northwestern University by Holman (2005) and predicted response from the extracted clay soil model in plane strain tests.

5. Data Integration: The myriad of heterogeneous data related to the development of underground space include a) design information, b) construction activities and images, c) monitoring data, and d) numerical model predictions. This data is not centrally located and thus poorly integrated. The integration of this data will provide all parties involved in the underground space development timely access to all relevant information and will facilitate informed decision making. The authors have used GIS (geographic information system) and augmented reality framework to integrate such heterogeneous datasets in 3-D and 4-d data bases. Figure 17 illustrate the various data streams integrated through this framework. A key feature of this integration is the development of a relational/flexible database. Conventional databases are typically developed for a predetermined set of data and applications. Thus, they feature rigid schemas with consistently formatted data. A flexible database has to conform to data of varying formats and styles. It must be capable of storing data of different formats from different sources within itself. The database must also be relational by providing handles to view and manipulate the data consistently and easily. This flexibility is especially required if the database interacts with data from distinct instances or events, but of the same underlying essence. Also, when the data is of multi-varied formats and schemas that need to be integrated and/or uniformly handled.

Figure 18 illustrates an instance of data integration and visualizations. The figure integrates geometric data including laser scan images of constructions stages, location of instruments, surrounding structures and support system. The various elements can be queried to provide information on the various objects include dimensions as well as instrument readings. Results of numerical model simulation and update are also integrated in this visual framework.

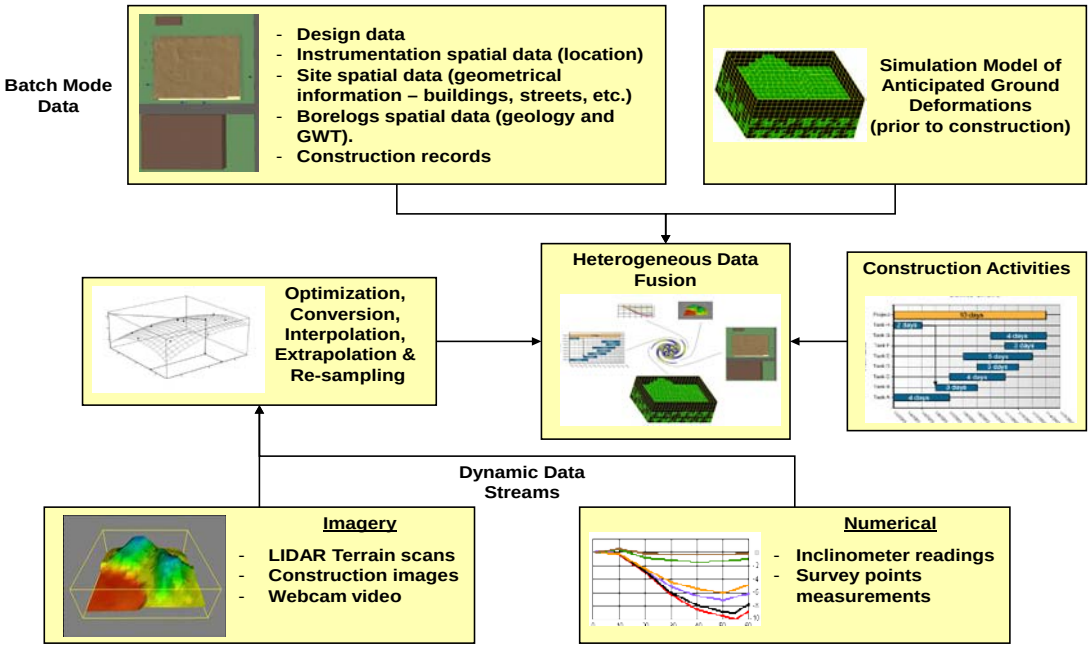

Figure 17: Heterogeneous data acquisition and integration.

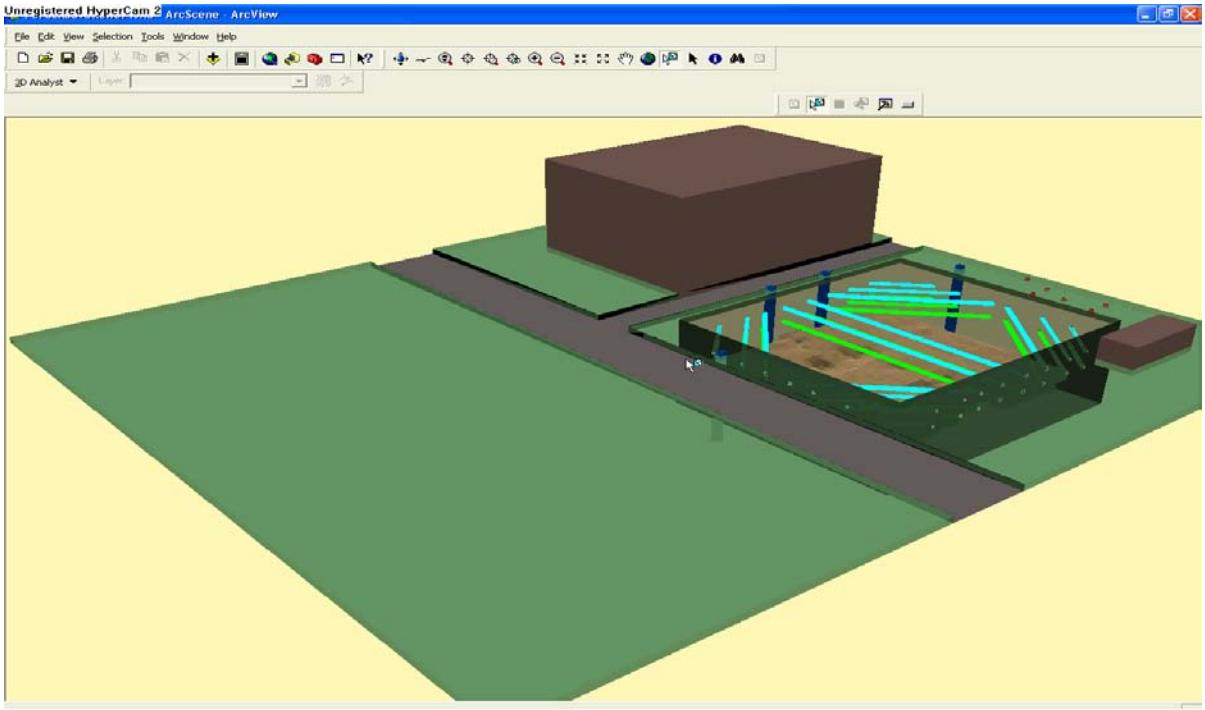

Figure 18: Feature based query through visualization of data integration.

6. Concluding Remarks: The paper describes novel developments of integrated tools to predict, monitor and control ground movements associated with supported excavations, including laser scanning and webcams for developing an accurate record of construction activities, automated and remote instrumentations to measure movements and structural responses, and intelligent, self-updating numerical models to compute anticipated ground movements. When systematically incorporated into a GIS based system, the resulting system has the potential to make the "observational approach" to excavation support a tool for the geo-industry. Successful use of monitoring data to update performance predictions of supported excavations depends equally on reasonable numerical simulations of performance, the type of monitoring data used as observations, and the optimization techniques used to minimize the difference between predictions and observed performance.

The calibration by inverse analysis of the various simulations presented herein indicated that the numerical methodology developed to optimize a finite element model of an excavation can be very effective in minimizing the errors between the measured and computed results. However, the convergence of an inverse analysis to an "optimal solution" (i.e. best-fit between computed results and observations) does not necessarily mean that the simulation is satisfactorily calibrated. A geotechnical evaluation of the optimized parameters is always necessary to verify the reliability of the solution. For a model to be considered "reliably" calibrated both the fit between computed and observed results must be satisfactory (i.e. errors are within desired and/or accepted accuracy) and the best-fit values of the model parameters must be reasonable.

The key to the successful calibration of an excavation lies in defining a "well posed" inverse analysis problem to calibrate the simulation. The parameters optimized by inverse analysis are few compared to the total number of parameters defining the behavior of the simulation. Indeed, the majority of the input parameters is estimated by conventional means and never "re-calibrated." Yet, the optimization can be extremely effective if a finite element simulation of the excavation adequately reproduces the stress history of the soil on site and the soil model adequately represented the behavior of the clays, at least in terms of appropriate field observations. In the cases presented herein with ground responses modeled by a conventional elasto-plastic soil model, the constitutive parameters that were relevant to the problem under study were calibrated based on inclinometer data obtained close to the support walls.

Acknowledgements: Financial support for this work was provided by National Science Foundation and the Infrastructure Technology Institute.

6. References:

[1] Anandarajah A. and Agarwal D. (1991). "Computer-aided calibration of soil plasticity model." *International Journal for Numerical and Analytical Methods in Geomechanics* Vol. 15, 835-856.

[2] Arai K., Ohta H. and Kojima K. (1986). "Application of back analysis to several test embankments on soft clay deposits." *Soils and Foundations*. Vol.26(2), 60-72.

[3] Burland, J.B. (1989). "'Small is beautiful' – the stiffness of soils at small strains: Ninth Laurits Bjerrum Memorial Lecture." *Canadian Geotechnical Journal*, Vol. 26, 499-516.

[4] Carter , J.P., Booker, J.R. and Small, J.C. (1979). "The analysis of finite elasto-plastic consolidation." *International Journal for Numerical and Analytical Methods in Geomechanics*, Vol. 3, 107-129.

[5] Calisto, L. and Calebresi, G. (1998). "Mechanical behavior of a natural soft clay." *Geotechnique*, Vol. 48 (4), 495-513.

[6] Calvello, M. (2002). "Inverse Analysis of a Supported Excavation through Chicago Glacial Clays," PhD thesis, Northwestern University, Evanston, IL.

[7] Calvello, M. and Finno R.J. (2002). "Calibration of soil models by inverse analysis." *Proc. International Symposium on Numerical Models in Geomechanics, NUMOG VIII*, Balkema, p. 107-116.

[8] Calvello M. and Finno R.J. (2003). "Modeling excavations in urban areas: effects of past activities." *Italian Geotechnical Journal*, 37(4), 9-23.

[9] Calvello M. and Finno R.J. (2004). "Selecting parameters to optimize in model calibration by inverse analysis." *Computers and Geotechnics*, Elsevier, Vol. 31, 5, 2004, 411-425.

[10] Chung, C.-K. and Finno, R.J. (1992). "Influence of Depositional Processes on the Geotechnical Parameters of Chicago Glacial Clays," *Engineering Geology*, 32, 225-242.

[11] Christian, J. T. and Wong, I.H. (1973). "Errors in simulation of excavation in elastic media by finite elements." *Soils and Foundations*, Vol. 13 (1), 1-10.

[12] Cho, W.J. (2007). "Recent stress history effects on compressible Chicago glacial clay," PhD thesis, Northwestern University, Evanston, IL.

[13] Clayton, C.R.I., and Heymann, G. (2001). "Stiffness of geomaterials at very small strains." *Geotechnique*, Vol. 51 (3), 245-255.

[14] Clough, G.W. and Mana, A. I. (1976). "Lessons learned in finite element analysis of temporary excavations." *Proceedings, 2nd International Conference on Numerical Methods in Geomechanics*, ASCE, Vol. I, 496-510.

[15] Clough, G.W. and Tsui, Y. (1974). "Performance of tied-back walls in clay." *Journal of the Geotechnical Engineering Division*, ASCE, Vol. 100 (12), 1259-1274.

[16] Clough, G. W., Smith, E.M., and Sweeney, B.P. (1989). "Movement control of excavation support systems by iterative design." *Current Principles and Practices, Foundation Engineering Congress*, Vol. 2, ASCE, 869-884.

[17] Finno, R.J., Atmatzidis, D.K., and Nerby, S.M. (1988). "Ground response to sheet-pile installation in clay," *Proceedings, Second International Conference on Case Histories in Geotechnical Engineering*, St. Louis, MO.

[18] Finno, R.J., Atmatzidis, D.K., and Perkins, S.B. (1989). "Observed Performance of a Deep Excavation in Clay," *Journal of Geotechnical Engineering*, ASCE, Vol. 115 (8), 1045-1064.

[19] Finno, R.J. and Blackburn, J.T. (2005). "Automated monitoring of supported excavations," *Proceedings, 13th Great Lakes Geotechnical and Geoenvironmental Conference, Geotechnical Applications for Transportation Infrastructure*, GPP 3, ASCE, Milwaukee, WI., 1-12.

[20] Finno R.J., Bryson L.S. and Calvello M. (2002). "Performance of a stiff support system in soft clay." *Journal of Geotechnical and Geoenvironmental Engineering*, ASCE, Vol. 128, No. 8, p. 660-671.

[21] Finno, R.J. and Calvello, M. (2005). "Supported excavations: the observational method and inverse modeling." *Journal of Geotechnical and Geoenvironmental Engineering*. ASCE, 131 (7).

[22] Finno, R.J., and Nerby, S.M., (1989). "Saturated Clay Response During Braced Cut Construction," *Journal of Geotechnical Engineering*, ASCE, Vol. 115, No. 8, 1065-1085.

[23] Finno, R.J. and Roboski, J.F., (2005). "Three-dimensional Responses of a Tied-back Excavation through Clay," Journal of Geotechnical and Geoenvironmental Engineering, ASCE, Vol. 131, No. 3, 273-282.

[24] Finno, R.J. and Tu, X. (2006). "Selected Topics in Numerical Simulation of Supported Excavations," *Numerical Modeling of Construction Processes in Geotechnical Engineering for Urban Environment*, International Conference of Construction Processes in Geotechnical Engineering for Urban Environment, Th. Triantafyllidis, ed., Bochum, Germany, Taylor & Francis, London, 3-20.

[25] Ghaboussi, J. and Pecknold, D.A. (1985). "Incremental finite element analysis of geometrically altered structures." *International Journal of Numerical Methods in Engineering*. Vol 20(11) 2061-2064.

[26] Gens A., Ledesma A., Alonso E.E. 1996. "Estimation of parameters in geotechnical backanalysis. - 2. Application to a tunnel excavation problem." *Computer and Geotechnics.* Vol. 18(1) pp.29-46.

[27] Gourvenec, S.M. and Powrie, W. (1999). "Three-dimensional finite element analysis of diaphragm wall installation." *Geotechnique*, Vol. 49(6), 801-823.

[28] Hashash, Y.M.A. (1992). "Analysis of deep excavations in clay," *Department of Civil and Environmental Engineering*. Ph.D. Thesis. Cambridge, MA: Massachusetts Institute of Technology, 337 p.
[29] Hashash, Y.M.A. and Finno, R.J. (2005). "Development of new integrated tools for predicting, monitoring and controlling ground movements due to excavations," *Proceedings, Underground Construction in Urban Environments*, ASCE Metropolitan Section Geotechnical Group, New York, NY,
[30] Hashash Y.M.A., Marulanda C., Ghaboussi J. and Jung, S. (2003). Systematic update of a deep excavation model using field performance data. Computers and Geotechnics, 30(6): p. 477-488.
[31] Hashash Y.M.A., Marulanda C., Ghaboussi J. and Jung, S. (2006). "Novel approach to integration of numerical modeling and field observation for deep excavation." *Journal of Geotechnical and Geoenvironmental Engineering*, Vol. 132(8), pp.1019-1031.
[32] Hashash, Y. M. A., Camilo Marulanda, Jamshid Ghaboussi, and Sungmoon Jung (2006) "Novel approach to integration of numerical modeling and field observations for deep excavations," *Journal of Geotechnical and Geoenvironmental Engineering*, Vol. 132, No. 8, pp 1019 - 1031.
[33] Hashash, Y.M.A., and A.J. Whittle (1996) "Ground movement prediction for deep excavations in soft clay," *Journal of Geotechnical Engineering*, Vol. 122, No. 6, pp 474-486.
[34] Hill, M. (1998). "Methods and guidelines for effective model calibration." *U.S. Geological Survey. Water-resources investigations report 98-4005*.
[35] Holman, T.P. (2005). "Small strain behavior of compressible Chicago glacial clay." PhD thesis, Northwestern University, Evanston, IL.
[36] Hughes, T.J.R. (1980). "Generalization of selective integration procedures to anisotropic and nonlinear media." International *Journal of Numerical Methods in Engineering*, Vol. 15 (9), 1413-1418.
[37] Jardine, R.J., Symes, M.J. and Burland, J.B. (1984). "The measurement of small strain stiffness in the triaxial apparatus." *Geotechnique*, Vol. 34 (3), 323-340.
[38] Koutsoftas, D. C., P. Frobenius, C.L Wu, D. Meyersohn, and R. Kulesza (2000). "Deformations during cut-and-cover construction of Muni Metro Turnback project," *Journal of Geotechnical and Geoenvironmental Engineering*, Vol. 126, No. 4, pp 344-359.
[39] Langousis, M.. (2007). "Automated Monitoring and Inverse Analysis of a Deep Excavation in Seattle," MS thesis, Northwestern University, Evanston, IL.
[40] Levasseur S., Malécot Y., Boulon M., Flavigny E., (2007). "Soil parameter identification using a genetic algorithm." *International Journal for Numerical and Analytical Methods in Geomechanics*, in press.
[41] Lings, M.L., Ng, C.W.W. and Nash, D.F.T. (1994). "The lateral pressure of wet concrete in diaphragm wall panels cast under bentonite." *Geotechnical Engineering*, Proceedings of the Institution of Civil Engineers, , 107, 163-172.
[42] Mana, A.I. and Cough, G.W. (1981). "Prediction of movements for braced cut in clay." *Journal of Geotechnical Engineering*, ASCE, New York, Vol. 107, No. 8, 759-777.
[43] O'Rourke, T.D. and Clough, G.W. (1990). "Construction induced movements of insitu walls." *Proceedings, Design and Performance of Earth Retaining Structures*, Lambe, P.C. and Hansen L.A. (eds). ASCE, 439-470.
[44] O'Rourke, T.D. and O'Donnell, C.J. (1997). "Deep rotational stability of tiedback excavations in clay," *Journal of Geotechnical Engineering*, ASCE, Vol. 123(6), 506-515.
[45] Ou, C.Y., Chiou, D.C. and Wu, T.S. (1996). "Three-dimensional finite element analysis of deep excavations." *Journal of Geotechnical Engineering*, ASCE, 122(5), 473-483.
[46] Ou C.Y., Tang Y.G. (1994). "Soil parameter determination for deep excavation analysis by optimization." *Journal of the Chinese Institute of Engineering*, Vol. 17(5)}, pp.671-688
[47] Peck R.B. (1969). "Deep excavations and tunneling in soft ground." *Proceedings, 7th International Conference of Soil mechanics and Foundation Engineering, State-of-the-ArtVolume*, 225-290.
[48] Poeter EP and Hill M.C. (1997). "Inverse Methods: A Necessary Next Step in Groundwater Modeling," *Ground Water*, Vol. 35, no. 2, 250-260.
[49] Poeter E.P. and Hill M.C. (1998). "Documentation of UCODE, a computer code for universal inverse modeling." U.S. *Geological Survey Water-Resources investigations report 98-4080*, 116 pp.
[50] Quiñones-Rozo, C. A., Y. M. A. Hashash, and L. Y. Liu (2008). "Digital Image Reasoning for Tracking Excavation Activities," *Automation in Construction*, Vol. 17, No. 5, pp 608-622.
[51] Sakurai S. and Takeuchi K. (1983). "Back analysis of measured displacements of tunnels," *Rock mechanics and rock engineering*, Vol.16, 173-180.
[52] Santagata, M., Germaine, J.T. and Ladd, C.C. (2005). "Factors Affecting the Initial Stiffness of Cohesive Soils." *Journal of Geotechnical and Geoenvironmental Engineering*, ASCE, Vol. 131(4), 430-441.
[53] Sabatini, P.J. (1991). "Sheet-pile installation effects on computed ground response for braced excavations in soft to medium clays." MS thesis, Northwestern University, Evanston, IL.

[54] Schantz, T., Vermeer, P.A. and Bonnier, P.G. 1999. "Formulation and verification of the Hardening–Soil Model." *R.B.J. Brinkgreve, Beyond 2000 in Computational Geotechnics.* Balkema, Rotterdam, 281-290.
[55] Stallebrass, S.E. and Taylor, R.N. (1997). "The development and evaluation of a constitutive model for the prediction of ground movements in overconsolidated clay." *Geotechnique*, Vol. 47 (2) 235-253.
[56] Su, Y.Y., Hashash, Y.M.A. and Liu, L.Y. (2006). "Integration of construction as-built data with geotechnical monitoring of urban excavation," *Journal of Construction Engineering and Management*, Vol. 132, No. 12, pp pp. 1234-1241.
[57] Trupp, T., Marulanda, C., Hashash, Y.M.A., Liu, L., and Ghaboussi, J., (2004). Novel methodologies for tracking construction progress of deep excavations. in Geo-Trans 2004. Los Angeles, CA.
[58] Tu, X. (2007). "Tangent stiffness model for clays including small strain non-linearity." PhD thesis, Northwestern University, Evanston, IL.
[59] Vorster, T.E.B., Mair, R.J., Soga, K., Klar, A. and Bennett, P.J. (2006). "Using BOTDR fibre optic sensors to monitor pipeline behaviour during tunnelling," Third European Workshop on Structural Health Monitoring, Granada
[60] Viggiani, G. and Tamagnini, C. (1999). "Hypoplasticity for modeling soil non-linearity in excavation problems." *Pre-failure Deformation Characteristics of Geomaterials*, M. Jamiolkowski, M, Lancellotta, R. and Lo Presti, D. (eds.), Balkema, Rotterdam, 581-588.
[61] Wakita, E. and Matsuo, M. (1994). "Observational design method for earth structures constructed on soft ground." *Géotechnique*. 44, No. 4, 747-755.
[62] Whittle, A.J. and Kavvadas, M.J. (1994). "Formulation of MIT-E3 constitutive model for overconsolidated clays." *Journal of Geotechnical and Geoenvironmental Engineering*, ASCE, Vol. 120(1), 173-198.
{63} Whittle, A.J., Y.M.A. Hashash, and R.V. Whitman (1993). "Analysis of deep excavation in Boston," *Journal of Geotechnical Engineering*, Vol. 119, No. 1, pp 69-90.
[64] Yamagami T., Jiang J.C., Ueta, Y. (1997). "Back calculation of strength parameters for landslide control works using neural networks." *Proceedings of the 9th Int. Conf. on Computer Methods and Advances in Geomechanics*, Wuhan, China.